IJE TRANSACTIONS C: Aspects Vol. 31, No. 12, (December 2018) 2044-2051

International Journal of Engineering

Journal Homepage: www.ije.ir

Fault Location on Compensated Transmission Lines without Current Measurement

K. Gorgani Firouzjah*

Faculty of Engineering & Technology, University of Mazandaran, Babolsar, Iran

PAPER INFO

Paper history:
Received 09 July 2018
Received in revised form 06 October 2018
Accepted 26 October 2018

Keywords:
Fault Location
Series Compensated
Synchronized Voltage Measurement
Current Transformer Elimination
Series Capacitor

ABSTRACT

This paper presents a novel fault location method for series compensated transmission lines. It is established based on synchronized voltages sampling and Thevenin impedance from both ends of series compensated transmission line. The method is based on the use of phasor measurement units (PMU) technology which is aimed to be independent of current measurements, fault type, fault resistance, fault inception angle and line loading angle. This method includes two subroutines for the faults located on the right and left sides of series capacitor (SC). Lumped modeling is considered for compensated transmission line with SC equipped with metal oxide varistor (MOV) arrester. The nonlinear behavior of SC-MOV system is investigated in the analysis. Proposed current independent fault location algorithm has been thoroughly tested using signals taken from simulations. According to the results, the percentage errors for the fault distances estimation are in proper ranges.

***doi**: 10.5829/ije.2018.31.12c.08*

1. INTRODUCTION

Compensated transmission lines with series capacitors (SC) brought several advantages to power system operations such as improving power transfer capability, transient stability and damping power oscillations [1]. In spite of these capabilities, series compensated lines have serious challenges regarding distance protection scheme. During fault occurrence and short circuit, system equations are affected by the nonlinear operation of parallel metal oxide varistor (MOV) as a protective unit of the series capacitor. Therefore, due to flow of high non-linear current through the line, the distance protection and fault location process have to be adapted.

Many fault location algorithms have been developed so far. The majority of them were performed by impedance measurement in fundamental power frequency. However, the non-linearity of MOV element affects the performance of the traditional impedance-based methods. The proposed solutions for this problem are series unit modeling that can be divided into empirical and analytical categories. One of the most used models in the fault location of series compensated lines is Goldsworthy's model [2]. Despite various attempts to different SC modeling techniques, this linearized approach is still considered and widely used.

Various algorithms for series compensated two-terminal lines have been analyzed in the literature. In some of them, the process is established based on impedance measurements. The impedance-based approaches can be categorized as one end [3, 4] and two ends [5-9] measurements. These techniques have to be adjusted to deal with the nonlinear characteristics of the MOV unit of the series compensator. These solutions include the use of fundamental frequency model of the series compensated line and single ended measurements [3], distributed time domain modeling of the transmission line and two ended synchronous sampling of voltages/currents [4]. A fault locating algorithm is proposed by Hussain and Osman [5] for compensated transmission lines using unsynchronized two-ended measurements. Post-fault data samples are used for data synchronization to improve the algorithm capability. Another method is proposed by junior et al. [6] for single and double-circuit series compensated lines which used voltages and currents measurements. This method is independent of fault resistance is performed by taking the differences of the voltages at both sides of

*Corresponding Author Email: *k.gorgani@umz.ac.ir* (K.G. Firouzjah)

Please cite this article as: K. Gorgani Firouzjah, Fault Location on Compensated Transmission Lines without Current Measurement, International Journal of Engineering (IJE), IJE TRANSACTIONS C: Aspects Vol. 31, No. 12, (December 2018) 2044-2051

the fault. Performance of the mentioned algorithm lead to low errors rates in different categories. A fault location strategy is carried out in literature [7] by lumped model of series compensated lines to avoid complexity without affecting accuracy. Apostolopoulos and Korres [8] presented a algorithm based on Phasor Measurement Units (PMUs) to deal with inter-circuit faults in double-circuit lines. This technique requires current measurement from both ends and the voltage only from one end.

The majority of fault location methods use the voltage and current samples to develop the algorithm and fault distance estimation. Current transformers (CT) and their undesired dynamic behavior under short circuits leads to certain construction limitations. The solution methods are aimed to make fault location algorithms independent of distorted secondary currents. The first remedies for assuring high accuracy under CT saturation can be performed by limiting the use of fault current phasors. The other remedies for CT saturation, except an intentional use of voltage signals, require identifying the CT saturation [10-12]. These algorithms are not independent of fault type and resistance.

Generally, the two-terminal location methods are more accurate than one-terminal methods and are able to minimize or eliminate the effects of fault resistance, loading, and charging current [13]. Faultlocation methods based on Synchronized Phasor Measurement are an interesting concept in the field of distance protection of transmission lines. There are a number of references that suggest using PMU for two-terminal cases [13]. Several methods based on synchronized phasor measurement are developed in literature [14-16] for Two–Terminal transmission lines. Due to CT inherent problems during fault interval, some new techniques based on synchronized voltage measurement have been presented in literature [17, 18]. Although the method was not independent of fault type and fault resistance. Firouzjah and Sheikholeslami [19] presented a method independent of fault type, fault resistance, and fault inception angle.

As mentioned above, this paper presents a fault location technique based on synchronized voltage measurement for series compensated transmission lines. The main objective is to present a method independent of measured signals with the current transformer. Simulationresults are presented to show the accuracy of proposed technique in different fault types. Also, different fault resistances are applied at different points.

2. PROPOSED FAULT LOCATING ALGORITHM

2. 1. Two Terminals Compensated Line at Pre-fault

Figure 1 shows a two-terminal series compensated line. The compensation process is done with a series capacitor protected by parallel MOV. E_{ThA}, Z_{ThA}, E_{ThB} and Z_{ThB} show Thevenin model from bus A and B respectively. l_{Right} and l_{Left} are the distances of capacitor's point from Buses A and B, respectively. Consequently, per unit distance from the Bus B is:

$$k_c = {l_{Right}}/{l_{line}} \tag{1}$$

Symmetrical components theory is used in order to transform three phase components (abc) to symmetrical components (with T matrix).

$$V^{012} = T^{-1}V_{abc} \qquad I^{012} = T^{-1}I_{abc} \tag{2}$$

$$Z^{012} = T^{-1}Z_{abc}T \qquad Y^{012} = T^{-1}Y_{abc}T \tag{3}$$

Consequently, Figure 1 can be illustrated in Symmetrical coordinate form as shown in Figure 2. Where, the superscript '012' denotes the symmetrical components which represent the zero, positive and negative sequences, respectively. E_{ThA}^{012} and E_{ThB}^{012} are Thevenin voltage sources of bus A and B, respectively. Regarding Figure 2, the procedure is proposed in Equations (4) to (7). As Equation (7), I_C is the pre-fault SC current matrix.

$$[V_{CA}^{012}] = [V_A^{012}] - (1-k_c)[Z^{012}]\left([Z_{ThA}^{012}]^{-1}([E_{ThA}^{012}] - [V_A^{012}]) - (0.5 - k_c/2)[Y^{012}][V_A^{012}]\right) \tag{4}$$

$$[V_{CB}^{012}] = [V_B^{012}] - k_c[Z^{012}]\left([Z_{ThB}^{012}]^{-1}([E_{ThB}^{012}] - [V_B^{012}]) - k_c[Y^{012}][V_B^{012}]\right) \tag{5}$$

$$[I_C^{012}] = \left([Z_{ThA}^{012}]^{-1}([E_{ThA}^{012}] - [V_A^{012}]) - (0.5 - k_c/2)[Y^{012}][V_A^{012}]\right) - (0.5 - k_c/2)[Y^{012}][V_{CA}^{012}] \tag{6}$$

$$[I_C^{012}] = \left([Z_{ThB}^{012}]^{-1}([E_{ThB}^{012}] - [V_B^{012}]) - (k_c/2)[Y^{012}][V_B^{012}]\right) - (k_c/2)[Y^{012}][V_{CB}^{012}] \tag{7}$$

2. 2. Two Terminals Compensated Line During Fault

A vast majority of fault location algorithms devoted to the series compensated lines have been established based on a two-stage analytical algorithm for distance protection. The fault analysis program is

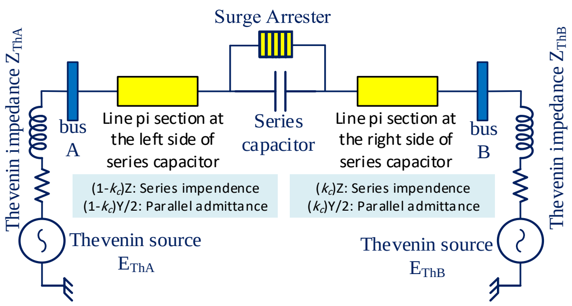

Figure 1. Single line diagram of typical compensated line

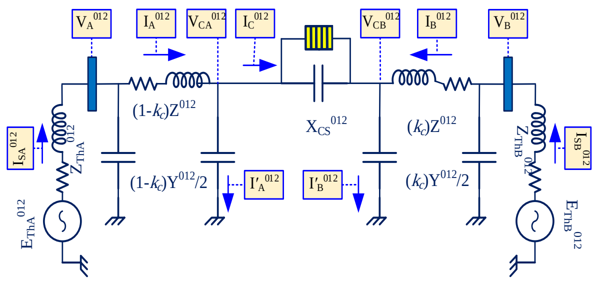

Figure 2. The π model of typical line in a symmetrical form

developed for the faults located on the left and right sides of SC. So, the algorithm is performed into two subroutines for the faults on the right and left sides of SC.

2. 2. 1. Faults on the Right Side of SC In this stage, the algorithm is performed for unknown faults occurred in right side of the capacitor. where, l_1 and l_2 are the distances from B and capacitor installation point to fault point, respectively. Thus, per unit fault distance from the B can be expressed as k_F:

$$k_F = l_1 / \quad , \quad 1 - k_F = l_2 / (k_c l_{line}) \tag{8}$$

According to Figure 3, the faulted line is divided into two π equivalent models. Figure 3 expresses the typical two-terminal network during fault on the basis of Thevenin equivalent circuit diagrams. In this figure, buses voltages have been considered as the difference between pre-fault and during-fault voltages. Thus, according to superposition theory, the current is the difference between during fault and pre-fault currents.

$$[\Delta V] = [\overset{f}{V}] - [\overset{\circ}{V}] \qquad [\Delta I] = [\overset{f}{I}] - [\overset{\circ}{I}] \tag{9}$$

Regarding Figure 3, ΔI_C can be calculated by Equation (10).

$$[\Delta I_C^{012}] = ([Z_{ThA}^{012}]^{-1} + (0.5 - k_c/2)[Y^{012}][V_A^{012}]) - \Big((0.5 - k_c/2)[Y^{012}]\Big([\Delta V_A^{012}](1 - k_c)[Z^{012}]\Big(-([Z_{ThA}^{012}]^{-1} + (0.5 - k_c/2)[Y^{012}][V_A^{012}])\Big)\Big)\Big) \tag{10}$$

For a compensated transmission line, a precise modeling of series capacitors and metal oxide varistors are required for any fault location algorithm. SCs and MOVs can be represented as fundamental-frequency equivalent in the form of resistance–capacitive reactance series branch for the algorithms based on the phasor technique. During fault interval, the capacitor current and consequently, its voltage drops rise to extremely high values. Thus, MOV starts conducting immediately after the instantaneous voltage across the capacitor exceeds a certain level. Thus, equivalent impedance of the compensator unit varies from capacitive to capacitive-resistive during fault interval. According to the capacitor fault current and capacitor protective current level (that is determined by the certain voltage level of the capacitor), the equivalent impedance is defined by Goldsworthy's model which is formulated as a function of SC current (I_C).

$$Z_{eq\,(I_C)} = R'_{C\,(I_C)} - jX'_{C\,(I_C)} \tag{11}$$

This model is modified by normalized SC current based on the capacitor protective level (I_{pr}).

$$I_{pu} = I_C / I_{pr} \tag{12}$$

$$Z_{eq\,(I_{pu})} = R'_{C\,(I_{pu})} - jX'_{C\,(I_{pu})} \tag{13}$$

The equivalent model is defined by Goldsworthy [2] as Equation (14). Where, X_{CS} is the nominal capacitor impedance.

$$\begin{aligned} &if\ I_C < 0.98 I_{pr} \rightarrow \{R'_C = 0\,, X'_{CS} = X_{CS} \\ &if\ I_C \geq 0.98 I_{pr} \rightarrow \\ &\begin{cases} R'_C = X_{CS}\left(0.0745 + 0.49e^{-0.243 I_{pu}} - 0.6e^{-1.4 I_{pu}} - 35e^{-5 I_{pu}}\right) \\ X'_{CS} = X_{CS}\left(0.1010 - 0.005749 I_{pu} + 2.088e^{-0.8566 I_{pu}}\right) \end{cases} \end{aligned} \tag{14}$$

Figure 3 shows a series compensator unit with the equivalent procedure. SC-MOV equivalent model is formulated using the compensator current during fault interval (I_c^f).

Regarding the superposition theory at Equation (9), this current can be obtained using Equations (7) and (10):

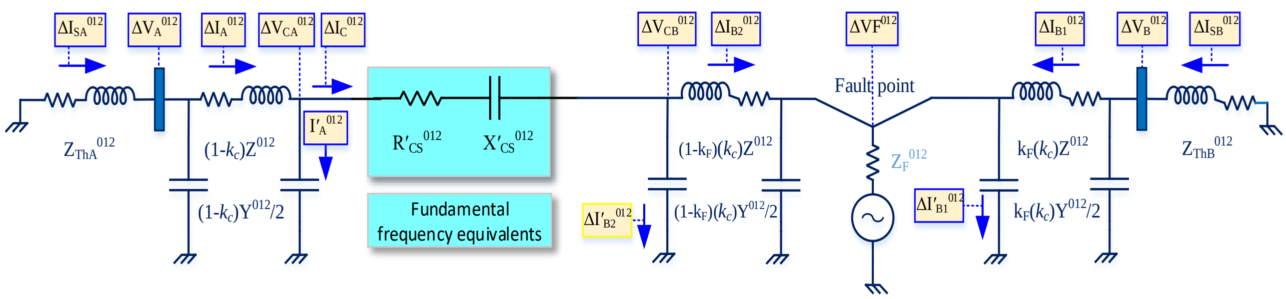

Figure 3. Thevenin equivalent model of the faulted system (Fault on the right side of SC)

$$[\overset{f}{I}_C] = [\overset{\circ}{I}_C] + [\Delta I_C] \quad (15)$$

The capacitor current in Figure 3 (ΔI_C) is determined based on the difference between during fault (I^f_C) and pre-fault capacitor currents (I°_C). Then, SC-MOV equivalent impedance is calculated and transferred to symmetrical form.

$$[I_{pu}] = [I_C^f / I_{pr}] \quad (16)$$

$$[Z_{eq}^{012}] = T^{-1}\left[diagonal\left(Z_{eq}^a, Z_{eq}^b, Z_{eq}^c\right)\right]T \quad (17)$$

Using this model, following relations are performed as Equations (18) to (20). The analytical process aims to calculate the fault point voltage (V_F) using system parameters as Equations (21) and (22).

$$[\Delta V_{CB}^{012}] = \left([\Delta V_A^{012}] - (1-k_c)[Z^{012}]\left(-\left([Z_{ThA}^{012}]^{-1} - (0.5 - k_c/2)[Y^{012}][\Delta V_A^{012}]\right)\right)\right) - [Z_{eq}^{012}][\Delta I_C^{012}] \quad (18)$$

$$[\Delta I_{B2}^{012}] = [\Delta I_C^{012}] - \left((0.5 - k_F/2)k_c[Y^{012}][\Delta V_{CB}^{012}]\right) \quad (19)$$

$$[\Delta I_{B1}^{012}] = -\left([Z_{ThA}^{012}]^{-1} + (k_F/2)k_c[Y^{012}]\right)[\Delta V_B^{012}] \quad (20)$$

$$[\Delta V_{F_L}] = \left(([I] - (0.5 - k_F/2)k_c[Y^{012}])[\Delta V_{CB}^{012}]\right) - \left((0.5 - k_F/2)k_c[Y^{012}][\Delta I_C^{012}]\right) \quad (21)$$

$$[\Delta V_{F_R}] = -k_F k_c[Z^{012}]\left([I] + [Z_{ThB}^{012}]^{-1} + (k_F/2)k_c[Y^{012}]\right)[\Delta V_B^{012}] \quad (22)$$

where, ΔV_{FL} and ΔV_{FR} are fault point voltage obtained using bus data on its left side (Bus A) and right side (Bus B), respectively. [I] is a 3-by-3 identity matrix. It is clear that the difference between these values must be minimized to zero. Therefore, the difference is defined as a final equation to obtain fault location as Equation (23). Where k_F value obtained using this equation is named as k_F^{Right}.

$$[\Delta V_{F_R}] - [\Delta V_{F_L}] = 0 \to f_{(k_F)} = 0 \to f_{Right(k_F)} = 0 \quad (23)$$

2. 2. 2. Faults on the Left Side of SC In order to analyze the faults on the left side of the SC, a hypothetical substitution has been used as follow. Similar to Figure 3, the faulted line is divided into two π equivalent models at two sides of fault point. Thus, similar to Equations (21) to (23), final relation to obtain fault distance on the left side of SC is as Equations (24) to (26). Where k_F value obtained using this equation is named as k_F^{Left}.

$$[\Delta V_{F_R}] = \left(([I] - (0.5 - k_F/2)(1 - k_c)[Y^{012}]^2)[\Delta V_{CA}^{012}]\right) - \left((0.5 - k_F/2)(1 - k_c)[Y^{012}][-\Delta I_C^{012}]\right) \quad (24)$$

$$[\Delta V_{F_L}] = -k_F(1 - k_c)[Z^{012}]\left([I] + [Z_{ThB}^{012}]^{-1} + (k_F/2)(1 - k_c)[Y^{012}]\right)[\Delta V_A^{012}] \quad (25)$$

$$[\Delta V_{F_R}] - [\Delta V_{F_L}] = 0 \to f_{(k_F)} = 0 \to f_{Left(k_F)} = 0 \quad (26)$$

2. 2. 3. Selecting the Fault Region with Respect to SC Regarding to Equations (23) and (26), k_F^{Right} and k_F^{Left} are obtained as fault location which is calculated based on the consideration of fault region with respect to SC. A recognizer algorithm for selecting either k_F^{Right} and k_F^{Left} as Figure 4 is proposed. In the practical application, there is no data about the fault region.The three phase voltage from the buses A and B are only the known signals.

Determination of fault side is depending on the values of the variables k_F^{Right} and $k_F^{Left}$from Equations (23) and (26). As shown in recognizer algorithm of Figure 4. If only one of these variables is in the range of [0,1], the fault is in its associated side. In the case of faults near SC, both k_F^{Right} and k_F^{Left} values are obtained in the [0,1] interval. Therefore, the fault side is determined by comparison of $f_{Right}(k_F)$ and $f_{Left}(k_F)$ in such a way that the fault occurs in the side which its objective function is lower. Therefore, each equation that is minimized in the lower value (ideally near to zero) results in the acceptable k_F value.

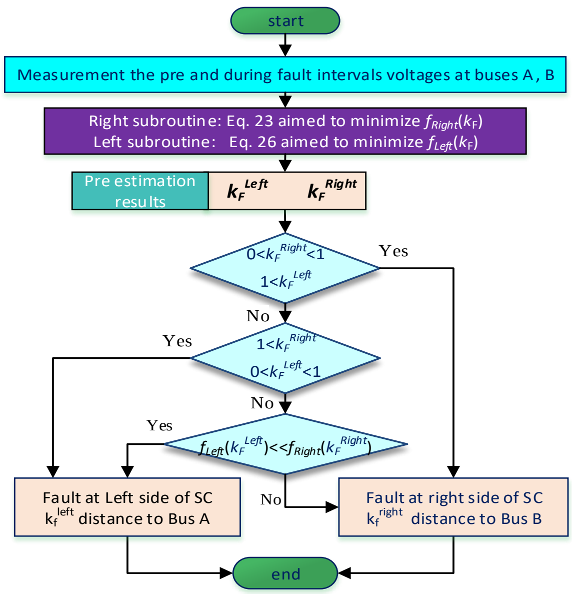

Figure 4. Detection of faulted section with respect to SC point

3. SIMULATION STUDY AND RESULTS ANALYSIS

Simulation for a 300 miles, 400 kV two–terminal transmission line was carried out. Table 1 shows the system parameters [20]. The simulations are established based on synchronized voltage phasor measurement of bus. The instantaneous voltages obtained from ATP/EMTP are applied to the Fourier transform. The fundamental power frequency component of the instantaneous voltages is used as voltage phasor.

In order to achieve a comprehensive evaluation of the proposed fault location method, it should be useful to consider following factors which affects the accuracy.

3. 1. Accuracy Evaluation Performing the fault location accuracy evaluation, different factors affecting the accuracy are taken into account. The main commonly changeable factors during the analysis are fault type, fault resistance, loading angle of the transmission line, fault inception angle and calculation of Thevenin impedance at both ends.

3. 1. 1. Fault Type and Resistance Transmission lines are subject to the unknown faults with various types and resistances. Hence, the proposed fault location algorithm must be independent of fault types and resistances variation. Simulation results have been presented in various fault types and resistances to validate the method. Figure 5 shows the percentage error of the fault location process with several faulttypes. The percentage error does not exceed 0.8%.

TABLE 1. System data used for the transmission line model

Transmission line Parameter	Positive/Negative sequence	$R^{+,-}$	0.249168	Ω /mile
		$L^{+,-}$	1.556277	mH /mile
		$C^{+,-}$	19.469	nF/mile
	Zero sequence	R^0	0.60241	Ω /mile
		L^0	4.8303	mH /mile
		C^0	12.06678	nF/mile
	Length	L	300	mile
	Voltage		400	kV
	Degree of compensation		75	%
	SClocation	l_{right}	150	mile
Thevenin Impedance		$ZSA^{+,-}$	17.177+j45.5285	Ω
		ZSA^0	2.5904+j14.7328	Ω
		$ZSB^{+,-}$	15.31+j45.9245	Ω
		ZSB^0	0.7229+j15.1288	Ω
MOV data		Reference current	44	kA
		Reference voltage	330	kV
		Exponent	23	

3. 1. 2. Loading Angle of the Transmission Line (δ) The line loading angle ($\delta = \delta_A - \delta_B$) is the factor that influences the algorithm. Hence, this method is tested by various loading angle (5 to 45°) in two fault types applied behind and front of SC. As Figure 6, the error does not exceed 1%. So, the method is almost uninfluenced by the line loading angle.

3. 1. 3. Fault Inception Angle Regarding the transient behavior of faulted system, it can be considered that maximum overvoltage and harmonic voltage will occur at voltage peak. The incepted faults at this time, lead to great transient state and changing fundamental frequency component of voltages. Figure 7 shows the error during the LG fault from 0 to 90-degree fault inception angles (α). According to this figure, the percentage error does not exceed 0.8%.

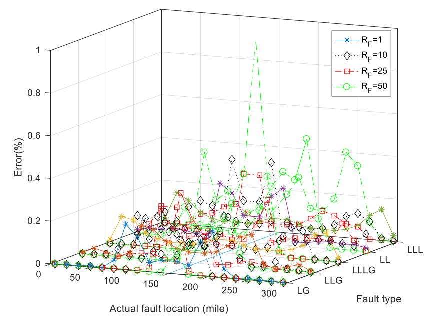

Figure 5. Percentage errors for various fault types

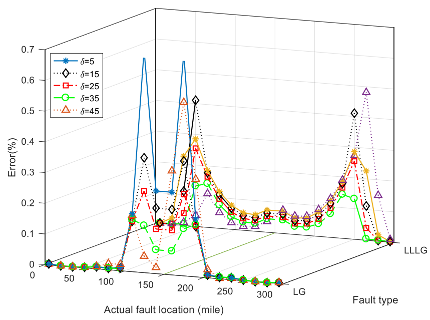

Figure 6. Percentage error for LLLG and LG faults located on the left and right sides of SC versus δ **(**R_{Fault}=10 Ω)

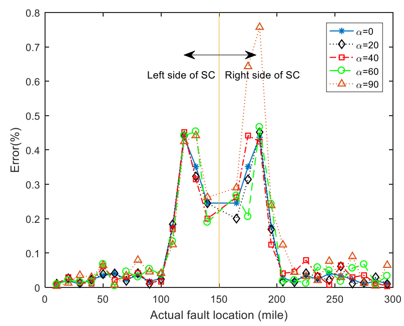

Figure 7. Percentage error for the LG faults versus (α)

3. 1. 4. Calculation of Thevenin Impedance at Ends The effectiveness of the method depends on the accurate calculation of the Thevenin impedance. Therefore, an appropriate sensitivity analysis of the method to variations of the Thevenin impedance must be applied.

In this way, sensitivity analysis of the method to variations of the Thevenin impedance and also calculation error of this impedance are simulated.

At the first, the Thevenin impedance is varied between 50 and 150% of the typical Thevenin impedance (see Table 1). It is assumed that the Thevenin impedance used in the simulation model and fault location algorithm is the same. In another word, the calculation error of the Thevenin impedance is not applied. Figure 8 shows the error for LLLG faults and various Thevenin impedance. The Thevenin impedance rate is defined as:

$$\frac{\text{Impedance}_{\substack{\text{Applied in algorithm}\\ \text{and simulation model}}} - \text{Impedance}_{\text{Typical value}}}{\text{Impedance}_{\text{Typical value}}} \times 100\% \qquad (27)$$

According to this definition, the Thevenin impedance rates varied between -50 and +50% of typical Thevenin impedance. As shown in Figure 8, the lower Thevenin impedances lead to lower fault location error left and right sides of SC versus Thevenin impedance variation. At the second process, the typical Thevenin impedance value is used in the simulation, but the value used in fault location process is varied between 80 and 120%.
In fact, the fault location algorithm is tested by calculation error of the Thevenin impedance:

$$\frac{\text{Impedance}_{\substack{\text{Applied}\\ \text{in algorithm}}} - \text{Impedance}_{\substack{\text{Typical value used}\\ \text{in simulation model}}}}{\text{Impedance}_{\substack{\text{Typical value used}\\ \text{in simulation model}}}} \times 100\% \qquad (28)$$

According to this definition, the calculation error of the Thevenin impedance varied between -20 and +20% of typical Thevenin impedance. The estimation error of the proposed algorithm for LLLG faults and various Thevenin impedance is shown in Figure 9.

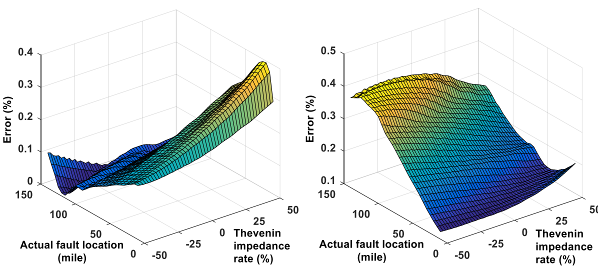

R_{Fault}=10 Ω left sides of SC R_{Fault}=10 Ω right sides of SC

Figure 8. Percentage error for the LLLG faults located on the left and right sides of SC versus Thevenin impedance error

3. 1. 5. SC Placed at One End of the Line In this section, compensation is studied for the case that one SC is located at one end of the line. Figure 10 shows the simulation results for the case that one SC is placed at bus A with different fault types and resistances. As this figure, the errors for studied cases are below than 0.04%.

3. 2. Discussion and Comparative Study Table 2 shows the comparison of the algorithm between proposed methods and also reported in literature [6-8, 17]. Results include maximum, minimum, mean and standard deviation amounts of fault location errors in different techniques for various fault resistances, inception angles and distances.The results verify the accuracy of the proposed algorithm. Note that this technique does not use information of CT during fault conditions. Regarding the accuracy evaluation of the proposed method, the main advantage is the fault location independent of current measurement. Inaddition, some benefits can be listed as:

- The process is uninfluenced by fault type (according Table 2, STD of the errors related to the five fault types are less than other methods), fault resistance (STD in Table 2), variation of line loading angle (Figure 6) and fault inception angle (Figure 7)
- Calculation of the Thevenin impedance at both ends could not able to change the estimation process. It means that technique is insensitive to source parameters of the system (Figures 8 and 9)

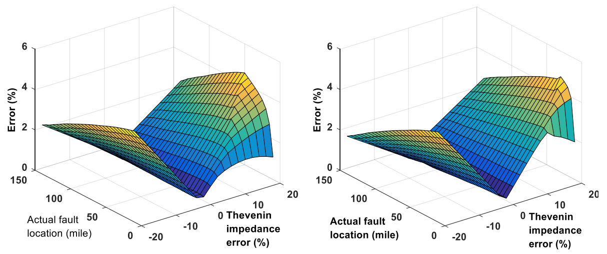

R_{Fault}=10 Ω left sides of SC R_{Fault}=10 Ω right sides of SC

Figure 9. Percentage error for the LLLG faults located on the left and right sides of SC versus Thevenin impedance error

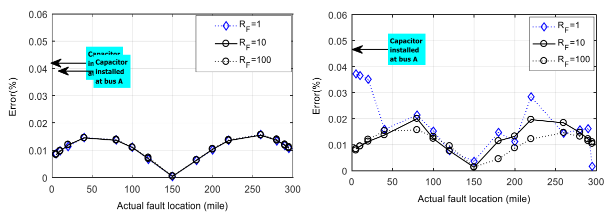

LG LLLG

Figure 10. Percentage error for the LG and LLLG faults with various resistances on the right side of SC (SC at bus A)

TABLE 2. Statistical results of the percentage error for the proposed algorithm compared to other related algorithms

Factor	Method	LG	LLG	LLLG	LL	LLL	Measurement v	Measurement i
Mean	Proposed	0.091	0.049	0.077	0.086	0.066	Y	N
	[6]	0.371	0.135	×	0.137	0.041	Y	Y
	[7]	4.623	1.513	×	3.396	5.277	Y	Y
	[7]*	1.513	8.738	×	6.008	2.270	Y	Y
	[7]**	8.738	0.924	×	3.506	4.112	Y	Y
	[8]*	0.088	0.168	0.205	0.263	0.228	Y	Y
	[8]**	1.411	1.739	1.344	0.969	1.292	Y	Y
	[17]	0.705	0.468	×	1.518	0.478	Y	N
STD	Proposed	0.139	0.088	0.113	0.110	0.070		
	[6]	0.196	0.104	×	0.125	0.027		
	[7]	3.996	1.398	×	4.242	4.860		
	[7]*	1.398	8.848	×	2.339	3.577		
	[7]**	8.848	1.588	×	3.912	3.677		
	[8]*	0.097	0.149	0.149	0.126	0.120		
	[8]**	0.870	0.935	0.591	0.269	0.437		
	[17]	0.628	0.300	×	1.135	0.241		

[7] * Takagi algorithm, ** Two end algorithm
[8]* Without (** Whit) considering measurement transformers
× there is no information about this fault type

4. CONCLUSIONS

In this paper, a new fault location method based on synchronized phasor measurement for Two–Terminal series compensated lines is presented. The proposed method estimates the fault location using the voltages of terminals at pre-fault and during-fault intervals. Series capacitor (SC) and metal oxide varistor (MOV) in series-compensated lines causes some difficulties for fault location. In order to develop the fault location algorithm, a linearized model based on empirical/practical results can be used instead of series compensator. The linearized resistive-capacitive equivalent impedance is considered as SC during fault interval. Different priorities are applied in this paper with respect to use the particular symmetrical components in the conventional Thevenin theory. The results indicate the accuracy of the algorithm with percentage error lower than 1%. Also, the proposed method recognizes the faulted section with respect to SC through two subroutines. The advantages of this method in comparison with the previous methods are CT elimination which makes the presented method independent of CT inherent problems. Fault location is independent of fault type, resistance, inception angle, line loading angles and source parameters.

5. REFERENCES

1. Abbasi, M., Shayestehkhah, H., and Tousi, B., "Application of an Additive Self-tuning Controller for Static Synchronous Series Compensator for Damping of Sub-synchronous Resonance Oscillations", ***International Journal of Engineering - Transactions A: Basics***, Vol. 31, No. 4, (2018), 564–573.
2. Goldsworthy, D.L., "A Linearized Model for Mov-Protected Series Capacitors", ***IEEE Transactions on Power Systems***, Vol. 2, No. 4, (1987), 953–957.
3. Saha, M.M., Izykowski, J., Rosolowski, E., and Kasztenny, B., "A new accurate fault locating algorithm for series compensated lines", ***IEEE Transactions on Power Delivery***, Vol. 14, No. 3, (1999), 789–797.
4. Sadeh, J., Hadjsaid, N., Ranjbar, A.M., and Feuillet, R., "Accurate fault location algorithm for series compensated transmission lines", ***IEEE Transactions on Power Delivery***, Vol. 15, No. 3, (2000), 1027–1033.
5. Hussain, S., and Osman, A.H., "Fault location on series and shunt compensated lines using unsynchronized measurements", ***Electric Power Systems Research***, Vol. 116, (2014), 166–173.
6. Manassero Junior, G., Di Santo, S.G., and Rojas, D.G., "Fault location in series-compensated transmission lines based on heuristic method", ***Electric Power Systems Research***, Vol. 140, (2016), 950–957.
7. Çapar, A., and Basa Arsoy, A., "A performance oriented impedance based fault location algorithm for series compensated transmission lines", ***International Journal of Electrical Power & Energy Systems***, Vol. 71, (2015), 209–214.
8. Apostolopoulos, C.A., and Korres, G.N., "Accurate fault location algorithm for double-circuit series compensated lines using a limited number of two-end synchronized measurements", ***International Journal of Electrical Power & Energy Systems***, Vol. 42, No. 1, (2012), 495–507.
9. Fulczyk, M., Balcerek, P., Izykowski, J., Rosolowski, E., and Saha, M.M., "Two-end unsynchronized fault location algorithm for double-circuit series compensated lines", In IEEE Power and Energy Society General Meeting - Conversion and Delivery of Electrical Energy in the 21st Century, IEEE, (2008).
10. Galijasevic, Z., and Abur, A., "Fault location using voltage measurements", ***IEEE Transactions on Power Delivery***, Vol. 17, No. 2, (2002), 441–445.
11. Pereira, C.E.M., and Zanetta, L.C., "Fault Location in Transmission Lines Using One-Terminal Postfault Voltage Data", ***IEEE Transactions on Power Delivery***, Vol. 19, No. 2, (2004), 570–575.
12. Xia, Y.J., Yin, X.G., Wang, Z.H., Yang, J.C., and Zhang, X.B., "A novel fault location scheme using voltage traveling-wave of CVTs", In 39th International Universities Power Engineering Conference, IEEE, (2004).
13. IEEE Std ,C37.11, IEEE Guide for Determining Fault Location on AC Transmission and Distribution Lines, (2005).
14. Joe-Air Jiang, Jun-Zhe Yang, Ying-Hong Lin, Chih-Wen Liu, and Jih-Chen Ma, "An adaptive PMU based fault detection/location technique for transmission lines. I. Theory and algorithms", ***IEEE Transactions on Power Delivery***, Vol. 15, No. 2, (2000), 486–493.
15. Joe-Air Jiang, Ying-Hong Lin, Jun-Zhe Yang, Tong-Ming Too, and Chih-Wen Liu, "An adaptive PMU based fault detection/location technique for transmission lines. II. PMU

implementation and performance evaluation", ***IEEE Transactions on Power Delivery***, Vol. 15, No. 4, (2000), 1136–1146.

16. Brahma, S.M., "New Fault-Location Method for a Single Multiterminal Transmission Line Using Synchronized Phasor Measurements", ***IEEE Transactions on Power Delivery***, Vol. 21, No. 3, (2006), 1148–1153.
17. Brahma, S.M., and Girgis, A.A., "Fault Location on a Transmission Line Using Synchronized Voltage Measurements", ***IEEE Transactions on Power Delivery***, Vol. 19, No. 4, (2004), 1619–1622.
18. Brahma, S.M., "Fault Location Scheme for a Multi-Terminal Transmission Line Using Synchronized Voltage Measurements", ***IEEE Transactions on Power Delivery***, Vol. 20, No. 2, (2005), 1325–1331.
19. Firouzjah, K.G., and Sheikholeslami, A., "A Current Independent Synchronized Phasor Measurement Based Method for Fault Location on Transmission Lines", In International Conference on Electrical Engineering, IEEE, (2007), 1–5.
20. Firouzjah, K.G., and Sheikholeslami, A., "A current independent method based on synchronized voltage measurement for fault location on transmission lines", ***Simulation Modelling Practice and Theory***, Vol. 17, No. 4, (2009), 692–707.

Fault Location on Compensated Transmission Lines without Current Measurement

K. Gorgani Firouzjah

Faculty of Engineering & Technology, University of Mazandaran, Babolsar, Iran

PAPER INFO

Paper history:
Received 09 July 2018
Received in revised form 06 October 2018
Accepted 26 October 2018

Keywords:
Fault Location
Series Compensated
Synchronized Voltage Measurement
Current Transformer Elimination
Series Capacitor

چکیده

در این مقاله روشی جدیدی برای محل¬یابی خطا در خطوط جبران‌شده سری ارائه شده است. روش ارائه‌شده بر پایه اندازه‌گیری ولتاژ دو پایانه خط و مدل تونن شبکه در دو انتها استوار شده است. فرمول‌بندی مسئله مبتنی بر تکنیک اندازه‌گیری ولتاژ است، به‌گونه‌ای که سهم مقاله را در عدم وابستگی روابط به جریان هنگام خطا مشخص می‌نماید. الگوریتم پیشنهادی در دو زیر الگوریتم پایه‌ریزی شده است. با روابط ارائه‌شده، در مرحله اول ابتدا سمت خطا نسبت به خازن شناسایی شده و سپس با استفاده از زیر الگوریتم مربوطه، تخمین محل خطا صورت می‌پذیرد. مدل‌سازی خط انتقال جبران شده در یک شبکه دو ترمینال و با ملاحظه رفتار غیرخطی عنصر جبران سازی موازی خازن (برق‌گیر) به انجام می‌رسد. راست آزمایی روابط و ارزیابی دقت تخمین محل خطا از طریق نتایج شبیه‌سازی صورت می‌پذیرد. قابلیت روش در بهره گیری از روابط کلاسیک با دقت و سرعت پردازش سریع است.

***doi**: 10.5829/ije.2018.31.12c.08*